

Experimental Dynamics of a Vortex within a Vortex

D. Durkin and J. Fajans

Department of Physics, University of California at Berkeley, Berkeley, California 94720-7300
(Received 28 June 2000)

We report the experimental dynamics of a new two-dimensional (2D) fluid phenomenon that occurs when an intense, pointlike vortex is placed within a diffuse, circular vortex. Our observations, made using strongly magnetized electron columns to model the 2D fluid, support the analysis performed by Jin and Dubin.

PACS numbers: 47.32.Cc, 47.15.Ki, 52.25.Gj

Two-dimensional (2D) fluid flows are common in nature; hurricanes, ocean eddies, Jupiter's Great Red Spot, and protoplanetary nebulae are intriguing examples. In the study of these flows, a number of fundamental vortex phenomena have been identified: the rollup of a vorticity filament into vortices via the Kelvin-Helmholtz instability; the mutual advection of vortices; the merger of two vortices; the axisymmetrization and filamentation of a vortex in a shear flow; the emergence and stability of a vortex pattern. Jin and Dubin recently identified a new 2D fluid phenomenon that occurs when an intense, pointlike vortex is placed within a diffuse, circular vortex (a disk of uniform vorticity) [1,2]. The pointlike vortex induces a wave on the disk's perimeter, which subsequently evolves into a vorticity hole within the disk. The hole is identical to an antivortex in the disk's rotating frame.

Figure 1 illustrates the dynamics of a vortex within a vortex. The black dot is the intense, pointlike vortex and the grey disk is the diffuse, circular vortex. In general, a vortex produces a rotational flow around its center, in a direction dependent on the vorticity's sign; the positive-vorticity dot and disk both generate a clockwise flow. Unperturbed, the disk would rotate uniformly (time is

measured in units of the disk's rotation period, τ). The dot, however, perturbs the disk's flow and distorts its perimeter, inducing a wave. The distorted perimeter self-consistently contributes to the wave's growth, and the wave eventually breaks (0.5τ). The hole being excavated in the disk's perimeter behaves as a negative-vorticity region superimposed upon the original positive-vorticity disk. This negative-vorticity region produces a counterclockwise flow, which draws vorticity from the disk and into a filament (1.0τ). The flow elongates the filament (2.0τ) and reattaches it to the disk, enclosing a vorticity hole (3.0τ). Then the dot's clockwise flow pulls the hole into the disk's interior (4.0τ). Thereafter the system behaves chaotically.

Figure 1, and all the figures and data herein, is obtained using strongly magnetized electron columns confined in a Malmberg-Penning trap (Fig. 2) to model the 2D fluid [3,4]. Under certain experimental conditions, the system behaves two dimensionally in the plane perpendicular to the imposed magnetic field \mathbf{B} , evolving by the $\mathbf{E} \times \mathbf{B}$ interaction where \mathbf{E} is the columns' self-electric field. This evolution is governed by equations identical to those that

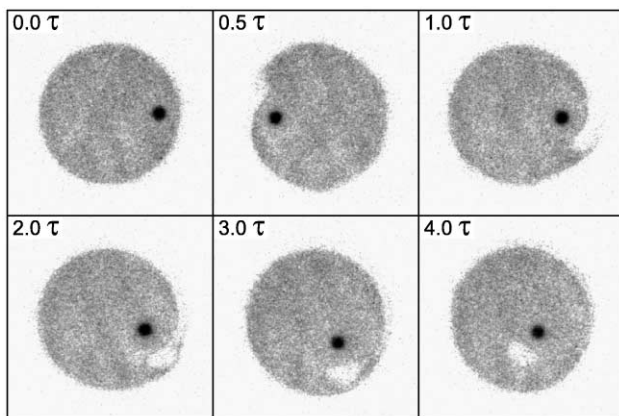


FIG. 1. The dynamics of a vortex (dot) within a vortex (disk). The dot induces a wave on the disk's perimeter, which then breaks (0.5τ) and spawns a filament (1.0τ). The filament elongates (2.0τ) and reattaches to the disk (3.0τ), enclosing a vorticity hole. The dot then pulls the hole into the disk's interior (4.0τ).

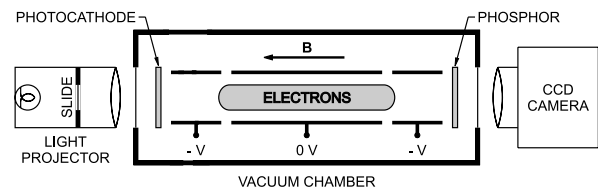


FIG. 2. The Malmberg-Penning Trap [12] consists of three coaxial, conducting cylinders contained within a high vacuum chamber. The electron columns are confined radially with a static magnetic field ($\mathbf{B} = 1$ T) and axially with electric fields ($-V$ is the confining potential). We create the desired initial 2D electron distribution by projecting the appropriate light image onto a cesium antimonide photocathode [13] and grounding the left cylinder; electrons are emitted only where there is light, and they stream along the magnetic field lines into the central confinement region, preserving their distribution. The electrons are confined by applying a negative electric potential to the left cylinder. The distribution is allowed to evolve for a given time, after which the right cylinder is grounded and the electrons are destructively imaged by streaming them onto a phosphor screen. A charge coupled device (CCD) camera detects the resulting image. The image's intensity is proportional to the electron density, and therefore to the vorticity.

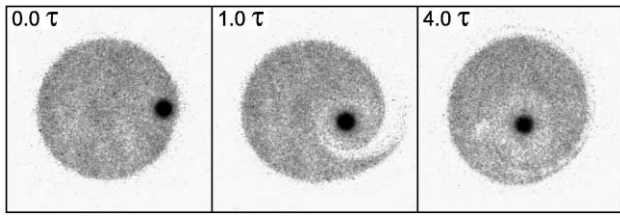


FIG. 3. The strong interaction of $R = 0.80$ and $\Gamma = 0.093$ leaves the dot centered inside the vorticity hole (4.0τ).

describe the behavior of an ideal 2D fluid. As electron density is equivalent to fluid vorticity, a strongly magnetized electron column is equivalent to a 2D fluid vortex.

Strongly magnetized electron columns are a valuable tool with which to study 2D fluids. Laboratory fluids are difficult to manipulate and diagnose, and are subject to undesired viscous and boundary effects. Numerical simulations, such as vortex-in-cell and contour dynamics, are computationally intensive, and are subject to numerical dissipation and discretization effects. Contour dynamics also fails when filaments form.

The dynamics of a vortex within a vortex depend on the dot's radial position (R) and circulation (Γ). R is normalized to the disk's radius; the disk's radius is fixed at $0.60 \text{ cm} = 0.3r_{\text{wall}}$, which is sufficiently far from the trap's wall that its influence is minimized (r_{wall} is the trap's wall radius). Γ is normalized to the disk's circulation and is given by $(nr^2)_{\text{dot}}/(nr^2)_{\text{disk}}$, where n is the electron density and r is the radius; the densities are fixed at $n_{\text{dot}} \approx 1.0 \times 10^7 \text{ cm}^{-3}$ and $n_{\text{disk}} = 1.8 \times 10^6 \text{ cm}^{-3}$. We vary Γ from 0.019 to 0.093 by changing the dot's radius.

The closer R is to one and the greater Γ , the stronger the interaction and the larger the induced wave's amplitude. For the intermediate interaction displayed in Fig. 1, R is 0.70 and Γ is 0.053. When the interaction is strong, as in Fig. 3 with $R = 0.80$ and $\Gamma = 0.093$, the dot dominates the flow and winds the disk's perimeter around itself, leaving the dot centered inside the vorticity hole. When the interaction is weak, the dot's influence may be insufficient to pull the hole from the disk's perimeter. Wave amplitudes smaller than 0.10 are suppressed entirely, consistent with an electron-temperature dependent, finite-column-length blurring effect unique to magnetized electron columns and not described by the 2D fluid-flow

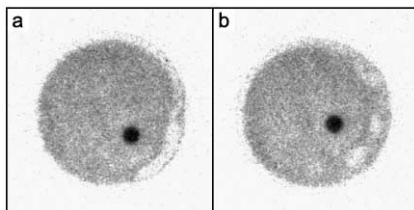


FIG. 4. Repeated hole formation for $R = 0.60$ and $\Gamma = 0.093$. (a) A new wave breaks inside the existing hole. (b) Three resulting holes.

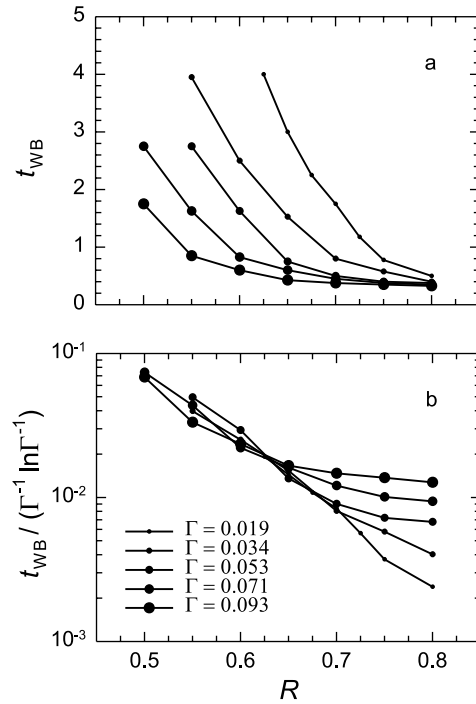


FIG. 5. (a) The time until a wave breaks, t_{WB} , versus R for five different Γ 's. (b) t_{WB} scaled by $\Gamma^{-1} \ln \Gamma^{-1}$ versus R .

Euler equations [5] (for $n = 2 \times 10^6 \text{ cm}^{-3}$, $T = 2 \text{ eV}$, and $L_p = 20 \text{ cm}$, the predicted blurring length is 0.05; the imaging resolution is 0.01).

When the dot remains close to the disk's perimeter after the hole has formed, the process may repeat, inducing a new wave (often within the existing hole) and generating another hole, as in Fig. 4. Such successive hole generation, however, is rare and not reproducible.

The time until the wave breaks (t_{WB}) is defined to be the time at which the perimeter's distortion develops a purely radial step. Figure 5(a) plots t_{WB} versus R for five different Γ 's. A notable feature of the data is that t_{WB} asymptotes to the same value for large R , independent of Γ . As the dot approaches the perimeter, the perimeter appears flat and passively advects in the dot's flow. In this limit, the wave breaks when nonlinear effects become significant; this occurs approximately when the circulation of the hole that is excavated from the original flat perimeter (Γ_{hole}) is equal to Γ_{dot} . We can estimate t_{WB} 's asymptotic value by placing the dot on the perimeter, as diagrammed in Fig. 6.

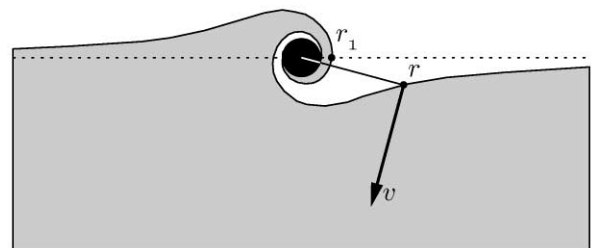


FIG. 6. Setup for calculating t_{WB} 's asymptotic value.

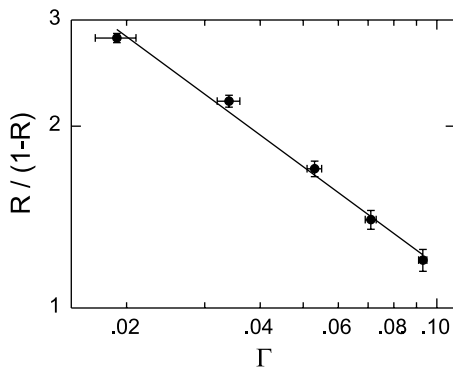


FIG. 7. The values of $R/(1 - R)$ versus Γ for when $t_{WB} = 1$. The line is the best fit.

At a distance r from the dot, a point will passively advect about the dot with velocity $v(r) = \Gamma_{dot}/(2\pi r)$. After a time t , the point has swept out an angle $\theta(r, t) = v(r)t/r$. Therefore,

$$\Gamma_{hole}(t) \approx n_{disk} \int_{r_1}^{r_2} \theta(r, t)r dr = \Gamma_{dot}(t/\tau)2 \ln(r_2/r_1),$$

where r_1 is given by the point labeled in Fig. 6 (note that it moves outward with time) and $\tau = 4\pi/n_{disk}$. Applying the condition that the wave breaks when $\Gamma_{hole} \approx \Gamma_{dot}$ yields

$$t_{WB} \approx \frac{\tau}{2 \ln(r_2/r_1)}.$$

We approximate r_2 as the point where $v(r_2)/v(r_1) = 0.1$, giving $r_2 = 10r_1$. Therefore, $t_{WB} \approx 0.2\tau$, consistent with our data.

Jin and Dubin mathematically analyzed the propagation of Kelvin waves on the disk's perimeter and thereby predict that, for $R < 0.7$, t_{WB} should scale as $\Gamma^{-1} \ln \Gamma^{-1}$. Our data, replotted in Fig. 5(b), support this scaling. Furthermore, they predict that when t_{WB} is equal to one, R and Γ should be related by $R/(1 - R) \sim \Gamma^{-\xi}$, where $\xi = 0.566$ as determined from contour dynamics simulations. We extract these values of R for each Γ from Fig. 5(a) and plot them in Fig. 7. The slope of the best fit line gives $\xi = 0.54 \pm 0.04$, in excellent agreement with predictions.

We now examine the dynamics of multiple vortices within a vortex and first consider the evolution of six symmetrically distributed dots within a disk, each with $R = 0.70$ and $\Gamma = 0.053$, in Fig. 8. As in the single dot case, each dot induces a wave and generates a hole. Each dot's flow carries its hole clockwise, moving it both inward and closer to the neighboring dot (2τ). The hole is then passed off to the neighbor (4τ), whose flow also carries it around clockwise, but now outward, ejecting the hole from the disk (10τ). The initial dot pattern is a known stable configuration, and it persists during the course of the evolution, though it decreases in size.

We next explore the evolution of an initially unstable dot pattern within a disk into a stable pattern via the vortex-

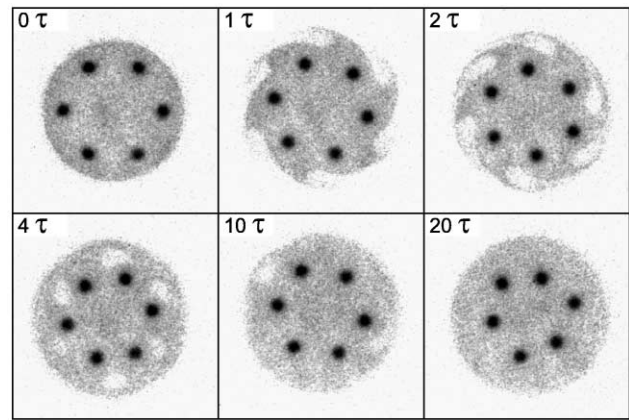


FIG. 8. Six dots within a disk. Each dot generates a hole, which, unlike in Fig. 1, is then expelled. The disk expands as the dots move inward, conserving the total angular momentum. The energy of the dots increases and the energy of the disk decreases, conserving the total energy; because the entropy of the disk also increases, this energy exchange is irreversible.

within-a-vortex phenomenon, a process relevant to the relaxation of 2D turbulence. In the relaxation of 2D turbulence, an initially turbulent vorticity distribution will coalesce into a number of intense vortices in a diffuse background of vorticity; the vortices chaotically advect, merge, and filament, often until one vortex or a positive and negative vortex pair remains [6]. Sometimes, however, the relaxation is arrested by the "crystallization" of the vortices into a stable pattern [7,8]. Jin and Dubin proposed that the vortices crystallize by exchanging energy with the background, and that the interaction described here ergodically mixes the background, making the energy exchange irreversible and maximizing the "regional fluid entropy" [9,10]. Vortex-in-cell simulations support this analysis [11]. To test this theory experimentally, we randomly placed seven dots (each with $\Gamma = 0.053$) within a disk; the dots quickly crystallized into a stable pattern (Fig. 9). Future experiments will study the crystallization's dependence on the disk's size, circulation, and uniformity.

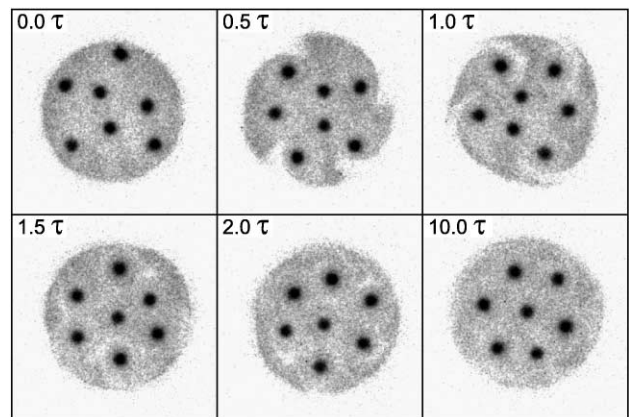


FIG. 9. Vortex crystallization. Seven initially randomly placed dots crystallize by interacting irreversibly with the disk.

We thank Dezhe Jin for suggesting this experiment. This work was supported by the Office of Naval Research.

-
- [1] D. Z. Jin, Ph.D. thesis, University of California, San Diego, 1999.
- [2] D. Z. Jin and D. H. E. Dubin (to be published).
- [3] R. H. Levy, Phys. Fluids **8**, 1288 (1965).
- [4] C. F. Driscoll and K. S. Fine, Phys. Fluids B **2**, 1359 (1990).
- [5] A. J. Peurrung and J. Fajans, Phys. Fluids B **5**, 4295 (1993).
- [6] J. C. McWilliams, J. Fluid Mech. **146**, 21 (1984).
- [7] K. S. Fine, A. C. Cass, W. G. Flynn, and C. F. Driscoll, Phys. Rev. Lett. **75**, 3277 (1995).
- [8] D. Durkin and J. Fajans, Phys. Fluids **12**, 289 (2000).
- [9] D. Z. Jin and D. H. E. Dubin, Phys. Rev. Lett. **80**, 4434 (1998).
- [10] D. Z. Jin and D. H. E. Dubin, Phys. Rev. Lett. **84**, 1443 (2000).
- [11] D. A. Schecter, D. H. E. Dubin, K. S. Fine, and C. F. Driscoll, Phys. Fluids **11**, 905 (1999).
- [12] J. H. Malmberg and J. S. deGrassie, Phys. Rev. Lett. **35**, 577 (1975).
- [13] D. Durkin and J. Fajans, Rev. Sci. Instrum. **70**, 4539 (1999).